

Catalysis Science & Technology

Accepted Manuscript



This is an *Accepted Manuscript*, which has been through the Royal Society of Chemistry peer review process and has been accepted for publication.

Accepted Manuscripts are published online shortly after acceptance, before technical editing, formatting and proof reading. Using this free service, authors can make their results available to the community, in citable form, before we publish the edited article. We will replace this *Accepted Manuscript* with the edited and formatted *Advance Article* as soon as it is available.

You can find more information about *Accepted Manuscripts* in the [Information for Authors](#).

Please note that technical editing may introduce minor changes to the text and/or graphics, which may alter content. The journal's standard [Terms & Conditions](#) and the [Ethical guidelines](#) still apply. In no event shall the Royal Society of Chemistry be held responsible for any errors or omissions in this *Accepted Manuscript* or any consequences arising from the use of any information it contains.

ARTICLE

Relationship between the anion/cation relative orientation and the catalytic activity for nitrogen acyclic carbene-gold catalysts

Cite this: DOI: 10.1039/x0xx00000x

Received 00th January 2012,
Accepted 00th January 2012

DOI: 10.1039/x0xx00000x

www.rsc.org/

L. Biasiolo,^{a,b,#} G. Ciancaleoni,^{b,#} L. Belpassi,^{b,*} G. Bistoni,^{b,c} A. Macchioni,^c F. Tarantelli,^c D. Zuccaccia^{a,*}

We elucidate the role of the ligand in determining the ion pair structure of the $[(\text{NAC})\text{Au}(\eta^2\text{-3-hexyne})]^+ \text{BF}_4^-$ [$\text{NAC} = \text{Nitrogen Acyclic Carbene}$, also known as $\text{ADC} = \text{Acyclic Diamino Carbene}$] catalysts and how the position of the anion influences their catalytic performances, giving a detailed relationship between the ion pairs structure, determined by ^{19}F , ^1H -HOESY NMR experiments and DFT calculations, and the catalytic activity in the intermolecular alkoxylation of alkynes. From our results, it is evident that if the anion is forced to be far from the catalytic site by ancillary ligand-anion hydrogen bonding interactions, the reaction slows down. On the contrary, if the anion is located near the alkynes the reaction is accelerated, coherently with the proposed active role of the anion in catalysis. These results open new opportunities in ligands design for the gold-mediated reactions in which the anion plays an important role during the catalysis.

Introduction

Ion pairing greatly affects many chemical reactions mediated by ionic transition-metal organometallic compounds¹ but finding a clear relationship between the anion/cation relative orientation in solution and the catalytic activity of charged complex is not an easy task.²

Concerning the catalysis of gold^{3,4} among the factors that influence the catalytic activity^{5,6,7} of a typical Au(I) cationic complex, the anion is demonstrated to be very important. Indeed, the number of papers focusing on the anion effect on yield,⁸ product distribution⁹ and the enantioselectivity¹⁰ of the catalyst is constantly growing. Moreover, the anion influences the structure of the catalyst¹¹ and important intermediates of the catalytic cycle.¹² A remarkable example highlighting the importance of ion-pairing has been reported by Toste and co-workers.^{10a} They showed that a high enantiomeric excess can be simply reached in the asymmetric hydroalkoxylation of allenes by the use of a chiral counterion. It was surmised¹³ that an even higher enantiomeric excess than reachable with a chiral auxiliary ligand might be achieved when chiral counterion resides near the catalytic site.

In order to shed some light on the anion effect, in the last years we have been carrying on a systematic NMR/DFT study on one of the key intermediates in the functionalization of double and triple C-C bonds, which is the linear bis-coordinated $[\text{LAu}(\text{UHC})]\text{BF}_4$ ion pair [$\text{UHC} = \text{unsaturated hydrocarbon}$, $\text{L} = \text{NHC}$, PR_3].¹⁴ We recently demonstrated, by combining ^{19}F , ^1H -HOESY NMR¹⁵ and relativistic Density Functional Theory

(DFT) calculations (Coulomb map potential and/or full ion pair optimization), how the anion/cation relative orientation can be finely tuned by the proper choice of the ligand¹⁶ and how the ion pair structure can be related with the electronic properties of the ligand (Scheme 1).

$$[\text{L}-\text{Au}-\text{UHC}]^+ \text{BF}_4^-$$

	L	Au	UHC
NHC	○○○		○
NHC(BIAN)	○○	○	○
PR ₃		○	○○○
PARF		○○○	○
P(OR) ₃			○○○○
NAC	?	?	?

Scheme 1. Relative abundances of different anion/cation orientations (near L, Au or UHC) for $[\text{LAu}(\text{UHC})]\text{BF}_4$ ion pair. $\text{UHC} = \text{alkenes and/or alkynes}$, $\text{NHC} = 1,3\text{-bis}(2,6\text{-diisopropylphenyl})\text{-imidazol-2-ylidene}$, $\text{NHC(BIAN)} = \text{bis(imino)acenaphthene-1,3-bis}(2,6\text{-diisopropylphenyl})\text{dihydroimidazol-2-ylidene}$, $\text{PR}_3 = \text{triphenylphosphine or tritertbutylphosphine}$, $\text{PARF} = 3,5\text{-bis}(2,4\text{-difluorophenyl})\text{phenylphosphine}$, $\text{P(OR)}_3 = \text{tris}(2,4\text{-diisopropylphenyl})\text{phosphite}$.

We already shown, for other transition metal complexes, that the anion may locate in a extremely defined position due to both steric¹⁷ and electronic¹⁸ sequestration.

Recently, we¹⁹ and others²⁰ studied the Au-catalyzed intermolecular alkoxylation^{21,22} of alkynes and proposed that the anion assists the nucleophilic attack of the methanol (the rate determining step, RDS) through the formation of a hydrogen bond, and it is not only a “proton shuttle”, as proposed in previous works.²³ Clearly, in order to exploit its role, the anion has to be located close to the unsaturated substrate.

This prompted us to search a relationship between the anion/cation relative orientation and the catalytic activity of gold complexes. For this reason, we synthesized four [(NAC)AuCl] (**P1-P4**) precatalysts (Scheme 2, NAC = Nitrogen Acyclic Carbene, also known as ADC = Acyclic Diamino Carbene),^{24,25} differing in the number and the position of the -OH and -NH moieties, and also in the steric hindrance around them, with the deliberate purpose of influencing the ion pair structure of the catalyst.

In particular, the structure of complex **P1** (Scheme 2) having a [NHR-(C=Au)-NHR]⁺ moiety recalls the urea and the guanidinium functional groups, two structures widely used for anion recognition.^{26,27} In complex **P2**, one nitrogen bears two *iso*-propyl groups, which create a steric hindrance around the -NH group, likely weakening the interaction with the anion. Complex **P3** is similar to **P2**, but the steric hindrance around the -NH is reduced. Finally, complex **P4** bears an additional -OH moiety, another suitable anchoring point for the anion introducing a competition between the amine and the alcoholic groups (Scheme 2).

In order to relate the ion pair structure and the catalytic activity, (i) we characterized the ion pair structure of the catalytically active species [(NAC)Au(η^2 -3-hexyne)]⁺ BF₄⁻ (**1-4BF₄**) by means of experimental (¹⁹F, ¹H-HOESY NMR) and theoretical (Coulomb maps, full ion pair optimization) techniques;

(ii) we investigated, by means of relativistic DFT calculation and Charge Displacement Function (CDF) analysis^{14,28,29} the gold-hexyne bond and the electron withdrawing ability of the metal fragment for **1-4BF₄** complexes;

(iii) we tested the catalytic performances of **P1-P4/AgX** (X⁻ = BF₄⁻, OTf⁻) in the alkoxylation of 3-hexyne with methanol in CDCl₃, where ion pairs are favoured, and in CD₃OD, where most of the organometallic salts are present as free ions.

Analyzing all these information, we found that the relative anion/cation orientation correlate with the catalytic performances of the catalysts **1-4BF₄**.

In particular in chloroform, if the anion is forced to be far from the catalytic site by ancillary ligand-anion hydrogen bonding interactions, the reaction slows down, coherently with the proposed active role of the anion during the catalysis.¹⁹ In methanol the weakly bound ion pairs (**2BF₄** and **4BF₄**) exhibit the same catalytic activity likely because they are completely dissociated, whereas in the presence of stronger anion/cation interactions (**1BF₄**) ion pairs are still present and show a smaller catalytic activity. This is in agreement with the fact that, according to our CDF results, ion pairs present a smaller electron withdrawing ability towards the unsaturated substrate (and consequently a reduced capability to activate the alkyne) than in corresponding free cation.

Results

Synthetic procedures. The neutral compounds **P1-P4** (Scheme 2) were synthesized using procedures similar to those reported in the

literature^{25f} (see Supporting Information for details). **1-4BF₄** complexes were generated in a NMR tube after the addition of AgBF₄ to a solution of neutral precursors **P1-P4** in the presence of 3-hexyne (solvent = CD₂Cl₂). All attempts to isolate complexes **1-4BF₄** failed and led to the formation of metallic gold. In the case of **3BF₄**, also the *in situ* characterization failed, due to the rapid decomposition of the complex to metallic gold, even at low temperature.

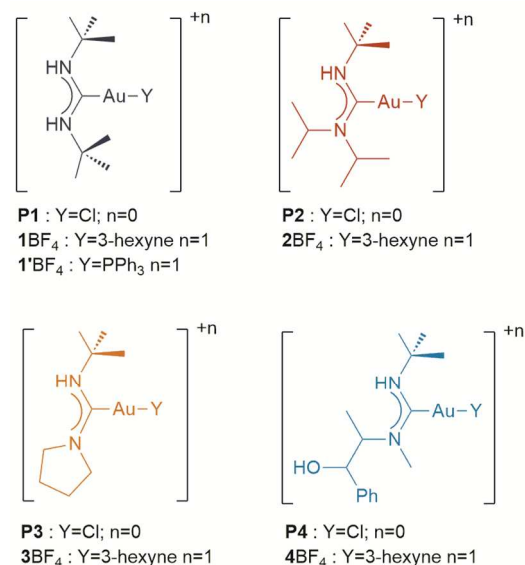
All the proton and carbon resonances belonging to the different fragments were assigned through ¹H, ¹³C, ¹H-COSY, ¹H-NOESY, ¹H,¹³C-HMQC NMR, and ¹H,¹³C-HMBC NMR spectroscopies (see Supporting Information).

The coordination of 3-hexyne to the [(NAC)Au]⁺ fragments causes a deshielding of the methylene (H2, see SI) resonance of 3-hexyne from 2.13 ppm (free) to 2.77, 2.79 and 2.74 ppm for **1BF₄**, **2BF₄** and **4BF₄**, respectively, as observed for similar compounds.^{16a, 16d}

The chemical shifts of quaternary carbon of 3-hexyne (C_{alk}) move from 80.96 ppm in the uncoordinated alkyne to 87.68, 88.14 and 87.90 ppm in **1BF₄**, **2BF₄** and **4BF₄**, respectively, as observed for similar NHC complexes^{16b, 16d}

Deshielding of the quaternary carbenic carbons (C_{carbene}) in **1BF₄**, **2BF₄** and **4BF₄** is between 2.9-3.6 ppm, respect to **P1**, **P2** and **P4**.

A marked difference in the presence of different rotamers of the carbene moiety in **P1** and **1BF₄** can be evidenced. In **P1**, as reported from Hashmi et al. for similar complexes, two different rotamers exist in solution (approximately 1:1 ratio), one of which is relative to the complex with the two *tert*-butyl groups pointing toward the gold (*syn-syn*), and the other one with one *tert*-butyl group in *anti* position to the gold (*syn-anti*).^{25f}



Scheme 2. Structure of **P1-P4**, **1-4BF₄** and **1'BF₄** complexes.

In the former the two sides of the carbene are magnetically equivalent and the two *tert*-butyl groups give only one NMR signal, whereas in the latter there is no symmetry and the two *tert*-butyl moieties give two different signals. On the contrary,

for 1BF_4 only the *syn-syn* rotamer existing, as proved by the presence of only one signal for the *tert*-butyl groups.

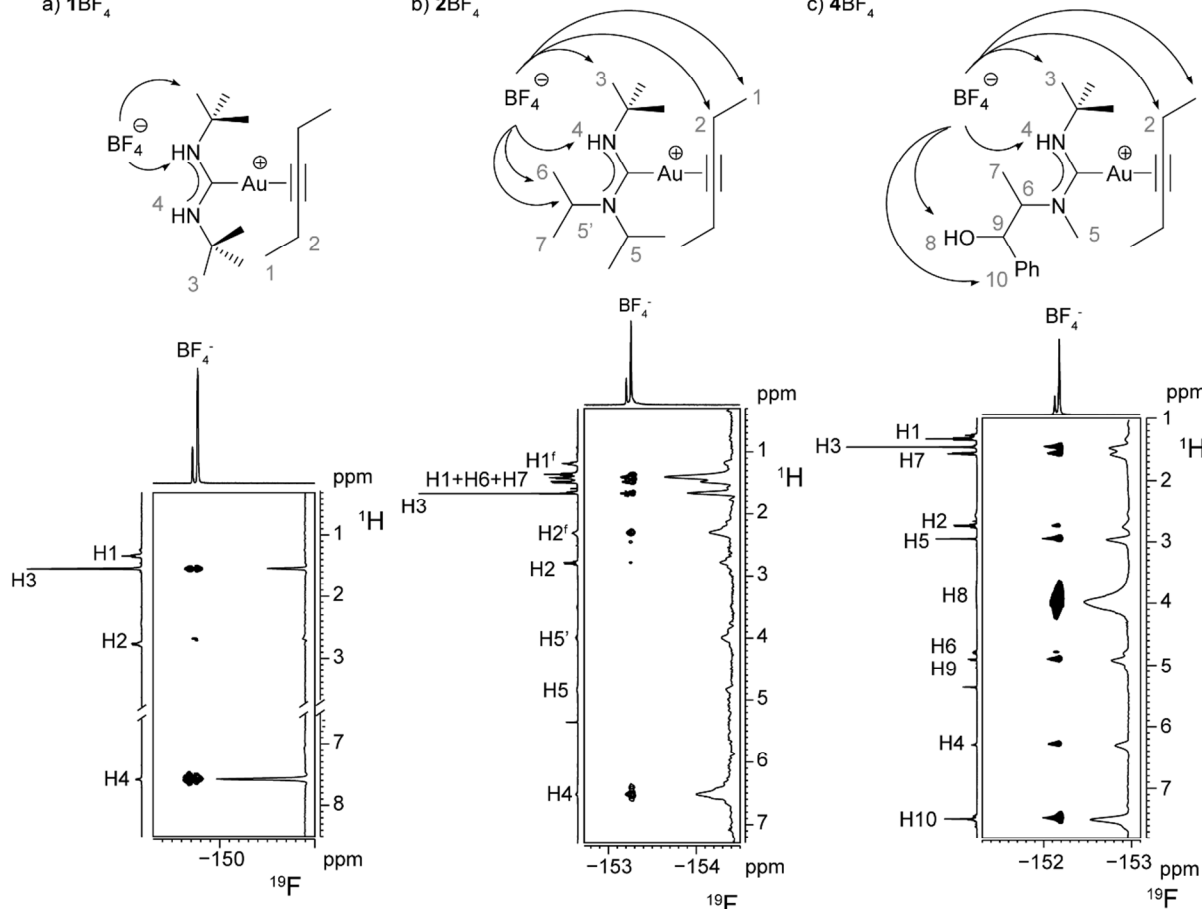
a) 1BF_4 b) 2BF_4 c) 4BF_4 

Figure 1. ^{19}F , ^1H -HOESY NMR spectrum (376.65 MHz, 298 K, CD_2Cl_2) of complexes 1BF_4 (a), 2BF_4 (b) and 4BF_4 (c). $\text{H}1^f$ and $\text{H}2^f$ are relative to the free 3-hexyne, in dynamic equilibrium with the coordinated one.

moiety is symmetrical. Nonetheless, such a rotation can be easily proved by ^1H EXSY (EXchange Spectroscopy) NMR (Supporting Information, Figure S2), while ^1H NMR NOESY experiments on **P3** does not show any indication of the rotation around the C-N(H)(Bu^t) bond at room temperature (Supporting Information, Figure S2).

It is interesting to note that the ^{19}F NMR chemical shift of BF_4^- strongly depends on the cation, being -149.7, -153.3 and -152.2 ppm for 1BF_4 , 2BF_4 and 4BF_4 , respectively. For comparison, the NMR resonances of the anion in $[\text{LAu}(\eta^2\text{-3-hexyne})]\text{BF}_4$ complexes, falls between -154 and -155 ppm (L = phosphine or NHC^{16a,d}).

Interionic NMR Studies. The relative anion/cation orientation in solution of 1BF_4 , 2BF_4 and 4BF_4 complexes has been investigated by ^{19}F , ^1H -HOESY NMR spectroscopy (Figure 1) in CD_2Cl_2 at room temperature.

^{19}F , ^1H -HOESY NMR spectrum of 1BF_4 exhibit a very strong contact between the fluorine nuclei of the BF_4^- and the protons directly bound to the nitrogen atoms (H4), a medium contact with the protons of the *tert*-butyl groups (H3), and very weak, almost undetectable, contacts with the 3-hexyne (H1 and H2) (Figure 1a). ^{19}F , ^1H -HOESY NMR spectrum of 2BF_4 show strong contacts between F atoms of the BF_4^- and the proton directly bound to the nitrogen atoms (H4), a medium contact with others protons of NAC ligand (H3, H6 and H7). In this

In the case of **P3**, a 180° rotation around the C-N(pyrrolidine) bond does not originate any rotamer because the pyrrolidine

case, also medium contacts with the 3-hexyne (H1 and H2) are observed (Figure 1b), making the NOE pattern much less selective than in the case of 1BF_4 . From the quantitative point of view, the H2/F contact is 8-fold less intense than the H4/F one (Table 1).³⁰ 4BF_4 has a hydroxyl group (H8) on one “side arm” of the carbene and an amine proton (H4), both of which are able to establish a hydrogen bond with the anion. The ^{19}F , ^1H -HOESY NMR spectrum clearly shows that H8/F is the most intense contact (Figure 1c), almost 8-fold more intense than H4/F. As in the case of 1BF_4 , the contact between the hexyne and the anion is very low, with a relative intensity of 0.03.

Table 1. Relative NOE intensities determined by arbitrarily fixing the largest NOE contact to 1.

Signal	Relative intensity		
	1BF_4	2BF_4	4BF_4
H1	0.01	0.12	0.02
H2	0.03	0.27	0.03
H3	0.11	0.25	0.06
H5	-	0.30	0.11
H4	1.00	1.00	0.13
H6	-	-	0.08
H7	-	0.18	0.11
H8	-	0.09	1.00

H9	-	-	0.11
H10	-	-	0.16

For comparison, it can be useful to remember that in the case of $[(\text{NHC})\text{Au}(\eta^2\text{-3-hexyne})]\text{BF}_4$ the most intense NOE contact is between the anion and the CH_2 on the backbone of the carbene, while the relative intensity of the NOE with the 3-hexyne is 0.4.^{16d}

In order to study the interaction between the anion and the carbene with two NH moieties in methanol, the ion pair structure of 1^+BF_4^- has been studied in deuterated methanol by ^{19}F , ^1H -HOESY NMR (see Supporting Information, Figure S3). We observe the same anion/cation orientation of 1BF_4 observed in CD_2Cl_2 and, even if the NH undergoes H/D exchange with the solvent and is, therefore, invisible in the NMR spectrum, the two *tert*-butyl groups are magnetically equivalent and present a weak NOE contact with the anion.

DFT studies. 1-4BF_4 have been thoroughly characterized by means of relativistic DFT calculations (see Supporting Information for all details). The full optimized structures for all complexes are reported in Supporting Information. All metal fragments ($[(\text{NAC})\text{Au}]^+$) show very similar interaction energies with the 3-hexyne (complexes 1^+-4^+), i. e. around 40 kcal/mol with variations of only 2.8 kcal/mol. The selected geometrical parameters describing the coordination mode of the 3-hexyne are also very similar. Note, for instance, that the deviation from linearity of the 3-hexyne, induced by the coordination to the metal center, is of 13 degrees for all complexes, suggesting that the nature of the interaction is very similar within these complexes.

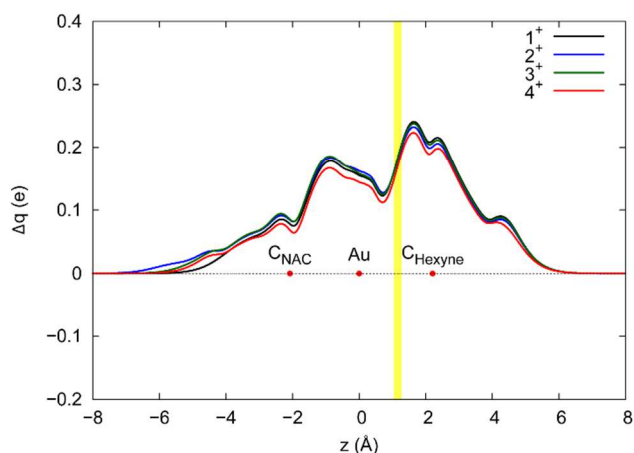


Figure 2. Charge displacement curves for the complexes 1^+-4^+ . The red dots represent approximate positions of the atoms. The vertical band identifies a suitable boundary between the metallic and the 3-hexyne fragments.

In order to study the variability of the chemical bonding features in the different NAC systems, we investigated the gold-substrate bond (complexes 1^+-4^+). In particular we use the analysis of the CDF^{28,29,14} ($\Delta q(z)$) that has been capable to give a detailed picture of the change in the electronic density due to the metal-carbon bond formation and a quantitative measure of the varying ability of different metal fragments to act as electron acceptor toward the unsaturated C-C bond of substrate (3-hexyne). The method is based on the partial integration along a chosen axis of the electron density difference between

the electron density of the complex and that of its non-interacting fragments placed in the same position they occupy in the complex. The fragments in our case are $[(\text{NAC})\text{Au}]^+$ moiety and the 3-hexyne (see Supporting for details) and the integration axis is defined as the axis joining the Au nucleus position and the midpoint of C-C triple bond of 3-hexyne. CDF defines at each point z the amount of electronic charge that, upon formation of the bond, has moved across a plane perpendicular to the axis through the point z . The results for 1^+-4^+ are reported in Figure 2. The overlapping of the four CDFs clearly shows that there is no significant differences between the Lewis acidity of different metal fragments. In particular, at the isodensity boundary (center of the vertical band in Figure 2), 0.18, 0.18, 0.17 and 0.17 electrons have been transferred from the hexyne to the $[(\text{NAC})\text{Au}]^+$ moiety upon the formation of the bond, for 1^+ , 2^+ , 3^+ and 4^+ , respectively. Noteworthy, the CDFs of all the complexes are practically identical also in the outer region of the 3-hexyne, where the nucleophilic attack is supposed to occur.

After the complete DFT characterization of the gold-substrate bond, we move on the interionic characterization of 1-4BF_4 ion pairs. Calculations were performed including explicitly the conductor like screening model (COSMO, $\epsilon = 8.93$) to include the solvent effect. The easiest way to rationalize the anion/cation relative orientation by DFT calculations is mapping the Coulomb potential of the sole cation,¹⁴ at least when small and weakly coordinating anions are used (BF_4^- in our case). Such maps for 1^+-4^+ cations (left side Figure 3) show clearly that H4 (the hydrogen bound to the nitrogen atom) is always one of the most attractive regions (blue colored) of the cation. In 2^+ , H4 is buried in the steric hindrance of the isopropyl group. In 4^+ , also H8 (the hydrogen bound to the oxygen) has a comparable Coulomb potential. On the other side, for all the complexes the protons of the hexyne (H2) are poorly attractive for the anion (Figure 3).

In order to quantify the energy difference between different ion pairs structures, the ion pairs 1BF_4 , 2BF_4 and 4BF_4 , have been fully optimized starting from several different geometrical configurations that only differ for the BF_4^- position (Figure 3). All calculations have been performed using the conductor like screening model (COSMO, $\epsilon = 8.93$, CH_2Cl_2) to include the solvent effect.

In the case of 1BF_4 , the anion is strongly bound to the NAC due to the presence of two H-bonds ($1\text{BF}_4\text{-a}$). The other accessible structure, that is the one with the anion in the alkyne position ($1\text{BF}_4\text{-b}$), is +4.6 kcal higher in energy. In the case of 2BF_4 , in which the NAC has only one hydrogen capable of giving hydrogen bond, the difference in energy between the structures with anion in the NAC and in the alkyne position is roughly halved, with the first that is however still the most stable configuration. Finally, in the case of 4BF_4 , we have found three possible optimized configurations, and in the most stable one the anion is close to the OH moiety ($4\text{BF}_4\text{-c}$). The latter is 3.9 kcal/mol more stable than the configuration having the anion interacting with the NH group ($4\text{BF}_4\text{-a}$) and 4.4 kcal/mol with respect to the configuration having the anion close to the alkyne ($4\text{BF}_4\text{-b}$) (Figure 3). In order to understand whether the anion may influence the activation of the π system, we investigated the impact of the anion on the Au-C bonding properties. We have worked out the CDFs for the systems $1\text{BF}_4\text{-a}$ and $2\text{BF}_4\text{-a}$. The corresponding CD curves are reported in Figure 4, together with the ones calculated for 1^+ and 2^+ (already discussed above). For the ion pairs, we have chosen the 3-hexyne and the remaining gold-ligand-anion moiety as fragments. The curves

clearly shows that the anion have a significant impact on the electron withdrawing ability of the metal fragment and so on the amount of charge that is subtracted from the 3-hexyne side.

At the boundary defined earlier, the amount of electronic charge passes

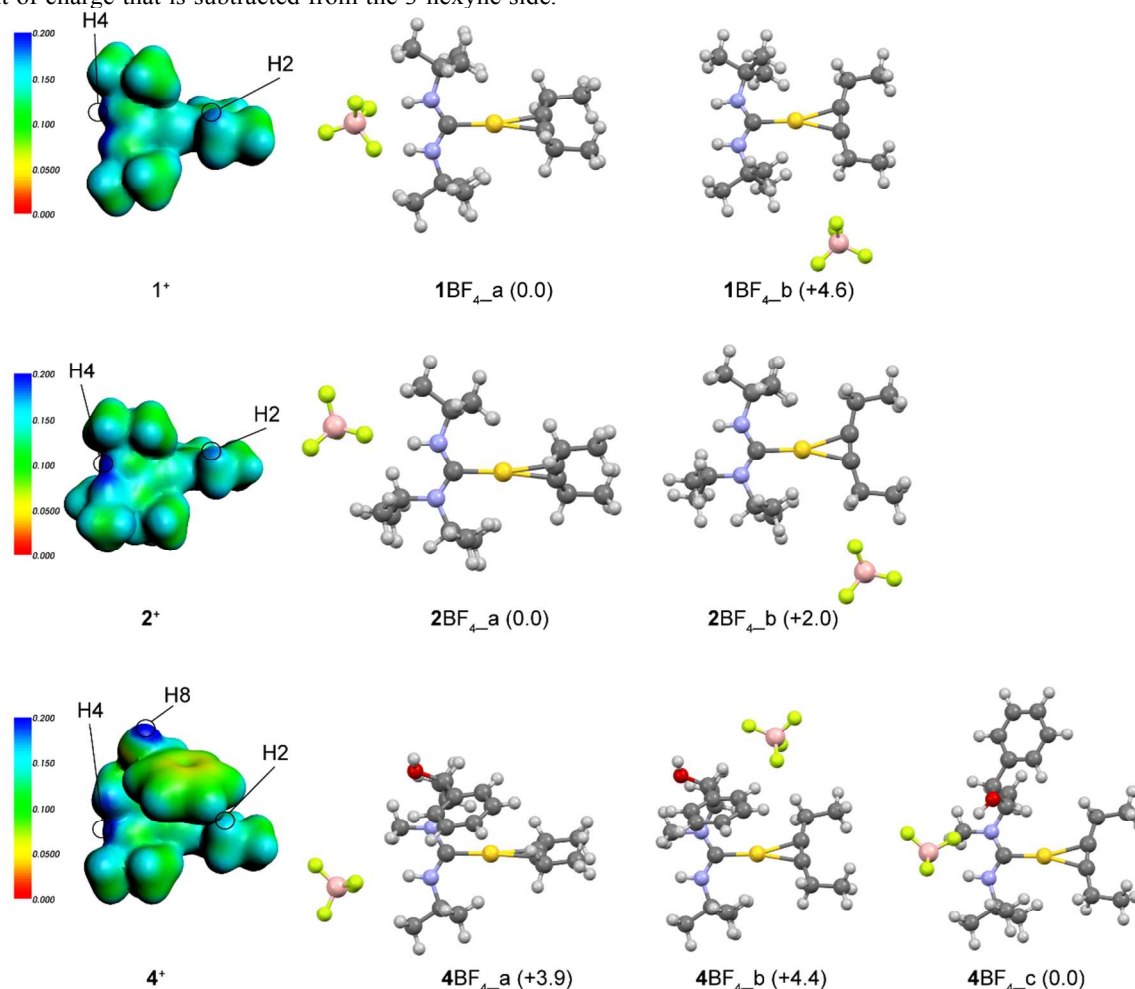


Figure 3. Left side: Color-coded representation of the Coulomb potential on an electronic isodensity surface ($\rho = 0.007 \text{ e/\AA}^3$) of the cationic complexes 1^+ , 2^+ and 4^+ . The regions corresponding to relevant part of the molecules are evidenced. Right side: DFT-optimized ion pair structures for the systems $1BF_4$, $2BF_4$ and $4BF_4$. The relative energies of the conformations are in parentheses and are expressed in kcal/mol.

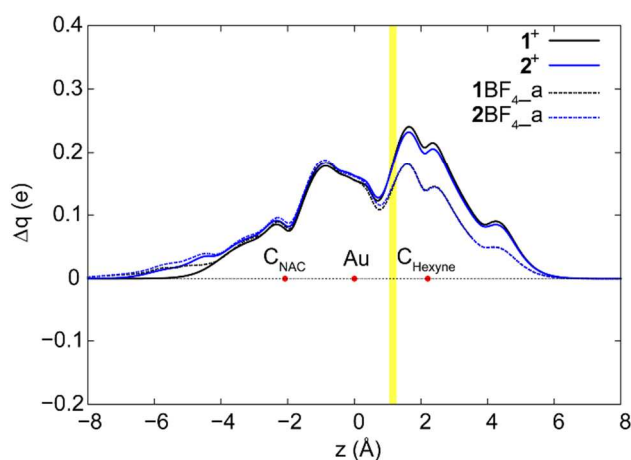
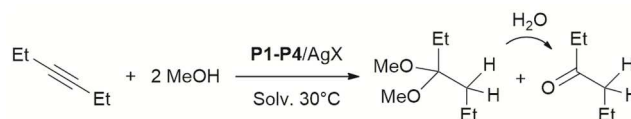


Figure 4. Charge displacement curves for the complex 1^+ , 2^+ , $1BF_{4_a}$, $2BF_{4_a}$. The red dots represent the approximate

position of the atoms. The vertical band identifies a suitable boundary between the metallic and the 3-hexyne fragments.

approximately from 0.18 to 0.14 in both cases going from the free cation to the ion pair structure (Figure 4).

Catalysis. Complexes **P1-P4** have been tested for the alkoxylation of 3-hexyne with methanol (Scheme 3), in the presence of different silver salts to generate the active catalyst *in situ*.



Scheme 3. Alkoxylation of 3-hexyne with methanol promoted by **P1-P4**/silver salt.

This reaction occurs at room temperature and can be conveniently monitored by NMR spectroscopy (see Supporting Information for details). Under these conditions it is known that the enol-ether resulting from the first attack of methanol on 3-hexyne is reactive and quickly undergoes the second attack of methanol leading to the formation of the 3,3-dimethoxyhexane.³¹ From the NMR spectra we observed also the presence of 3-hexanone, the product of the hydrolyzation of the 3,3-dimethoxyhexane due to the traces of water. A typical catalytic run was ruled out mixing, 3-hexyne and methanol in the presence of the catalyst precursor (1% in mol) and a silver salt (1% in mol) at 30 °C in CDCl₃ or CD₃OD.

P1/AgBF₄, **P3**/AgBF₄ and **P4**/AgBF₄ reaches similar conversions (24-30%) in 90 minutes (entry 1, 4 and 5, Table 2), whereas catalyst **P2**/AgBF₄ reaches 59% in the same time (entry 2, Table 2) using CDCl₃ as solvent (Figure 5). It is interesting to note that the catalytic rate of **P3**/AgBF₄ decreases slowly after the first hour, when the conversion is just 20%. Comparing the value of the initial turnover frequency TOF₃₀ (calculated after 30 minutes), we can see that catalysts **P1**/AgBF₄, **P3**/AgBF₄ and **P4**/AgBF₄ are almost similar while catalyst **P2**/AgBF₄ is two time faster (entries 1, 4, 5 and 2 respectively, Table 2).

When the catalysis is carried on using **P2**/AgBF₄ as catalyst and N,N'-Dicyclohexylurea (DCU) as additive, the reaction rate decreases reaching a value similar to catalysts **P1**/AgBF₄, **P3**/AgBF₄ and **P4**/AgBF₄ (compare entry 3 with entries 1, 4 and 5, Table 2).

Table 2 - Gold(I) catalysed alkoxylation of 3-hexyne

Entry	Cat.	AgX	Conv. (Yield) [%] ^[c]		TOF ₃₀ [min ⁻¹] ^[d]
			90 min	180 min	
1	P1	BF ₄ ⁻	24 (21)	43 (34)	0.30
2	P2	BF ₄ ⁻	59 (55)	91 (87)	0.83
3 ^[a]	P2	BF ₄ ⁻	33(26)	54(48)	0.35
4	P3	BF ₄ ⁻	28 (23)	44 (37)	0.43
5	P4	BF ₄ ⁻	30 (20)	52 (42)	0.36
6	P1	OTf ⁻	50 (47)	77 (73)	0.73
7	P2	OTf ⁻	83 (79)	99 (96)*	1.60
8	P3	OTf ⁻	58 (44)	84 (69)	0.88
9	P4	OTf ⁻	57 (54)	91 (88)	0.66
10 ^[b]	P1	BF ₄ ⁻	20 (11)	37 (24)	0.26
11 ^[b]	P2	BF ₄ ⁻	75 (68)	99 (94)*	1.06
12 ^[b]	P3	BF ₄ ⁻	39 (34)	62 (56)	0.43
13 ^[b]	P4	BF ₄ ⁻	77 (71)	97 (90)*	1.23

Catalysis conditions: 30 °C, 3-hexyne (100 μL), Cat/AgX (1 mol%), CH₃OH (143 μL), CDCl₃ (400 μL), [a] performed with 5 mol% of N,N'-Dicyclohexylurea as additive, [b] CD₃OD (543 μL). [c] Conversions and TOF₃₀ were determined by ¹H NMR spectroscopy, using TMS as internal standard, as average of three runs. [d] TOF₃₀ = (n product / n catalyst)/(30 min). * the catalysis reached full conversion before 180 min.

Discussion

Ion pairs structure. The anion/cation relative position have been studied experimentally, by ¹⁹F, ¹H-HOESY NMR, and theoretically, by means of Coulomb potential maps and ion pair optimizations. The different degree of selectivity in the HOESY spectra of **1BF**₄, **2BF**₄ and **4BF**₄ makes clear that the ion pair structures of the three compounds are markedly different. A convenient way to describe such structures for linear gold(I) salts is to quantify the two main structures, with the anion close to the

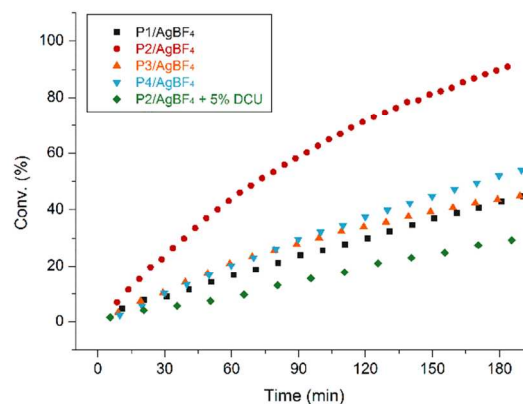


Figure 5. Alkoxylation of 3-hexyne with methanol catalyzed by **P1**-**P4** complexes activated with AgBF₄ in CDCl₃.

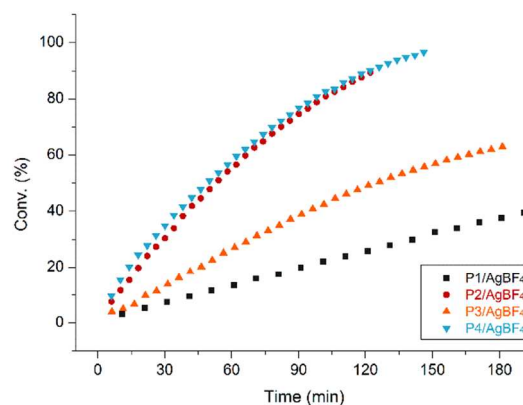


Figure 6. Alkoxylation of 3-hexyne with methanol catalyzed by **P1**-**P4** complexes activated with AgBF₄ in CD₃OD.

ancillary ligand (structure A) or to 3-hexyne (structure B), as already reported for similar complexes.¹⁶

Specifically, **1BF**₄ shows an exceptional ion pair selectivity, with the anion interacting almost exclusively with the two -NH¹⁸ of the NAC (Figure 1), and an A:B ratio of 97:3 can be calculated.³² The high stability of this ion pair structure can be easily explained by the presence of two cooperating hydrogen bonds, forming a cyclic structure similar to that formed by guanidinium-based anion receptors,^{26,27} in which two fluorine atoms of the anion interact with the two coplanar N-H moieties. The presence of such a strong interaction is evidenced also by the NMR shift of the fluorine nuclei (-149.7 ppm) which is considerably lower than that with other ligands. Moreover, the supramolecular cycle given by the two hydrogen bonds stabilizes the *syn-syn* structure so much to make the C-N

rotational barrier insurmountable at room temperature and inhibiting the formation of the *syn-anti* rotamer, as experimentally evidenced. DFT studies fully confirm this structure, evidencing a very attractive potential on the NH region (Figure 3) and a large energy difference between the DFT-optimized $1BF_4$ _a and $1BF_4$ _b (4.6 kcal/mol, Figure 3). The spectrum of 1^+BF_4 in methanol- d_4 demonstrates that the anion-cation interaction is so strong to exist also in a polar solvent as methanol (see Supporting Information, Figure S3). In fact, also in this case the *syn-anti* rotamer is not present and NOE contact between BF_4^- and the two equivalent *tert*-butyl groups is consistent with the ion pair structure of $1BF_4$ in CD_2Cl_2 . Consistently, it is known that in the case of the cationic guanidinium-like structures $(HN-CR-NH)^+$, as the one present in $1BF_4$ and 1^+BF_4 , the two cooperative hydrogen bonds with an anion are so strong that the methanol is generally not enough to break the ion pair.^{27,33}

In the case of $2BF_4$, which has only one -NH moiety, the ^{19}F , 1H -HOESY NMR is much less selective (Figure 1), and the H2/F contact is clearly visible and measurable. In this case, the A:B ratio can be estimated as 79:21. The latter is very similar to those previously obtained for complex $[(NHC)Au(\eta^2\text{-3-hexyne})]BF_4$.^{16d} Looking at the DFT-optimized structure of the cation, the -NH still presents a very attractive potential (Figure 3), but it is partially buried in the steric hindrance of the isopropyl group bound to the other nitrogen. This is reflected on a smaller difference of energy between the DFT-optimized structures $2BF_4$ _a and $2BF_4$ _b (2.0 kcal/mol, Figure 3).

For the last compound, $4BF_4$, having a hydroxyl group on one arm of the carbene, the most intense NOE contact is between the anion and the -OH (Figure 1). In this case the A:B ratio is not enough anymore to exhaustively describe the ion pair structure in solution, but adding the configuration with the anion close to the hydroxyl group (C), and using H8/F, H4/F and H2/F as probes for the ratio of the configurations, the A:B:C ratio is 11:3:86. This is in good agreement with DFT studies, according to which the -NH and -OH regions have similar attractive potentials, but the -OH is less sterically hindered than the -NH. As a consequence, DFT-optimized conformation $4BF_4$ _c is the most stable one, by 3.9 and 4.4 kcal/mol with respect to $4BF_4$ _a and $4BF_4$ _b, respectively.

Interestingly, the ^{19}F NMR shift nicely correlates with the anion/cation specific interactions present in solution: indeed, it is -149.7 for $1BF_4$ (two $-NH \cdots F-BF_3$ interactions), -152.2 ppm for $4BF_4$ (one strong $-OH \cdots F-BF_3$ interaction), -153.3 ppm for $2BF_4$ (one weak $-NH \cdots F-BF_3$ interaction) and between -154 and -155 in absence of hydrogen bonding interactions.¹⁶

Unfortunately, the low stability of $3BF_4$ did not allow us to experimentally characterize its ion pair structure, but the corresponding Coulomb map (Supporting Information, Figure S4) allows us to predict it: the -NH is again the most attractive region of the cation and a good $-NH \cdots F-BF_3$ interaction can be expected. The pyrrolidine cycle on the other nitrogen creates some steric hindrance around the -NH, but less than the isopropyl group in $2BF_4$. For this reason, we expect an A:B ratio intermediate between those of $1BF_4$ and $2BF_4$.

Catalysis. The ion pairs structure and the alkyne-gold bond in **P1-P4/AgX** catalysts are expected to be of key importance in the RDS of the alkoxylation, namely the nucleophilic attack of the first molecule of methanol on the triple bond. It has been already reported on the role of the anion during such step,^{18,19} demonstrating that it establishes a hydrogen bond with the alcoholic proton of the methanol, which results activated.

Obviously, in order to do that, the anion must be located close to the 3-hexyne. On the other hand, the acidity of the $[LAu]^+$ fragment is important to activate the triple bond: the more acidic the metal fragment is, the more electronic density is transferred from the alkyne to the gold, likely with a proportional $C \equiv C$ activation.^{31,34}

Our detailed DFT studies demonstrate that all the considered cations behave similarly in the interaction with 3-hexyne. In particular they present the same electron withdrawing ability towards 3-hexyne with an almost identical alkyne \rightarrow gold net donation. Remarkably, also the amount of gold \rightarrow alkyne back-donation, which can be qualitatively estimated by the alkyne bending²⁹ (Supporting Information), seems to be the same for all the systems. If we also consider that the geometry of the attack is *anti*-periplanar and, consequently, there is no direct interaction between the methanol and the steric hindrance of the ligand, this electronic similarity of 1^+-4^+ cations suggests that they would activate the 3-hexyne with the same efficiency and should catalyze the alkoxylation of hexyne with the same performances. Assuming this hypothesis, we can ascribe every difference in the catalytic performances to the anion.

Comparing catalytic and HOESY results, a trend appears evident: the complexes for which a strong anion-ligand hydrogen bond is possible (i.e. $1BF_4$, $3BF_4$ and $4BF_4$) have similar and low catalytic rates. On the contrary, the complex in which the hydrogen bond donor is sterically hindered and shows the lowest A:B ratio ($2BF_4$) has also the highest catalytic performances. This is consistent with the *scenario* depicted previously, according to which the anion has a beneficial role in activating the methanol lowering the activation barrier of the attack: if a specific interaction, stronger than the anion/methanol one, keeps the anion far from the catalytic center, it cannot play its role of activator and the reaction slows down.

Using *N,N'*-Dicyclohexylurea (DCU), which possesses a functional group able to interact with the counterion (BF_4^-), as additive with the catalyst **P2/AgBF₄**, it likely keeps the anion far from the catalytic centre, slowing down the catalysis and giving performances similar to those of **P1/AgBF₄** and **P4/AgBF₄**.

An additional proof of the anion role comes from the comparison of OTf^- instead of BF_4^- as anion: activating the pre-catalysts with $AgOTf$ there is a systematic increase of the performances of two/three times (compare entries 1, 2, 4, 5 with 6,7 8, 9 in Table 2) in chloroform. The increase of the TOF_{30} values are due to the fact that more basic anions can activate the methanol to a higher degree,¹⁹ but the trend among the considered catalysts is the same.

Using methanol as solvent instead of chloroform usually produces the separation of organometallic ion pairs in free ions.³⁵ Analyzing the catalytic results in methanol, it is evident that **P2/AgBF₄** and **P4/AgBF₄**, whose TOF_{30} values were very different in $CDCl_3$, have now the same activity. Since the corresponding active species, $2BF_4$ and $4BF_4$, are likely present in methanol as free ions,³⁶ and since DFT studies revealed that 2^+ and 4^+ have the same acidity (Figure 2), their similarity in catalyzing the reaction is reasonable and confirms that the differences in $CDCl_3$ were due to the anion.

On the other hand, **P1/AgBF₄**, bearing a guanidinium-like moiety, shows lower TOF_{30} values in CD_3OD with respect to those of **P2/AgBF₄** and **P4/AgBF₄**. NMR studies confirm that, differently from $2BF_4$ and $4BF_4$, $1BF_4$ is likely present as an ion pair having the anion close to the -NH moieties. The acidity of the gold in the ion pair is smaller than in the cation (Figure 4),

due to the “neutral” character of the complex, therefore the alkyne will be less activated and less prone to the nucleophilic attack of the methanol. **P3**/AgBF₄ shows a catalytic activity that is intermediate between those of **P1**/AgBF₄ and **P2**/AgBF₄. Since the corresponding Coulomb potential map of **3BF**₄ (Supporting Information, Figure S4) indicates that the -NH moiety is more exposed and more prone to the interaction with the anion than in the case of **2BF**₄ and **4BF**₄, we can expect that **3BF**₄ is present in solution as a mixture of free ions and ion pairs, giving an intermediate activity.

Conclusions

In conclusion, we have shown that the ion pair structure of gold complexes in solution can be tuned by modifying the functional groups of the NAC ligand, and, more important, differences in ion pairs structure dramatically influence the catalytic performances of the NAC-gold catalysts. In particular if the anion is forced to be far from the catalytic site by ancillary ligand-anion hydrogen bonding interactions, the rate of alkoxylation of 3-hexyne by methanol slows down. On the contrary if the anion is located near the alkynes the reaction is accelerated, coherently with the proposed active role of the anion in catalysis.

Detailed information on ion pair structure have been obtained by combining NOE NMR experimental studies and theoretical DFT calculations. Two main orientations were observed: one with the anion close to the carbene backbone (A), the other one with the anion close to the methylene moiety of the 3-hexyne (B). The A:B ratio can be estimated by comparing different NOE contacts and it goes from 97:3, when two synergic hydrogen bonds are involved (**1BF**₄), to 79:21, when the -NH attractive region of the cation is partially hindered by the surrounding bulky groups (**2BF**₄). But the versatility of NAC ligands allows also to break this “two configurations rule” observed also in our previous paper: **4BF**₄ bears an hydroxyl group on one arm of the acyclic carbene, introducing a third ion pair configuration, which is particularly stable for the hydrogen bond between the -OH and the anion (orientation C).

DFT calculations allowed us to give insights on the ion pair structures and to make sure, by the CDF approach, that the **1-4**⁺ cations have the same acidity, in order to ascribe any variation in the catalytic activity to the different ion pair structure.

As a test reaction, we selected the alkoxylation of 3-hexyne by methanol, for which the turnover limiting step is supposed to be the nucleophilic attack of the methanol to the coordinated 3-hexyne. We recently proposed that in the transition state of the nucleophilic attack of the first methanol, the latter is “activated” by a hydrogen bond with the anion. However, in order to exploit this role, the anion has to be present in the orientation B. Activating **P1-P4** with different silver salts (AgBF₄ and AgOTf) in chloroform, we found that the TOF₃₀ can be well related to the percentage of “orientation B” found for the **1-4BF**₄ complex, and the best performing catalyst is the one having the weakest interaction between the NAC and the anion (**2BF**₄).

In methanol, the complexes **1-4BF**₄ cannot be characterized because they readily react with the solvent, but **P2** and **P4**, once activated with AgBF₄, give the same catalytic activity, as expected by considering that the anion is likely not anymore bound to the cation and that **2**⁺ and **4**⁺ have the same ability to activate the 3-hexyne. Conversely, **1BF**₄ shows a lower catalytic activity, which can be explained by the two following facts: i) methanol is not polar enough to break the two strong

cooperative hydrogen bonds that exist between anion and cation in **1BF**₄, as confirmed by ¹⁹F, ¹H- HOESY NMR experiments conducted for parent **1**⁺BF₄, and ii) the acidity of a neutral ion pair is lower than that of a cation.

Finally, in this work we have elucidated the role of the ligand in determining the ion pair structure of the complexes and how the latter influences the catalytic performances of the catalyst, giving a detailed relationship between ion pairs structure and catalytic activity. This opens new opportunities in ligands design for the gold-mediated reactions in which the anion plays an important role during the catalysis. We are currently exploring the possibility to optimize chemical processes through the control of the anion-cation interactions, and either computational and experimental studies are underway in our laboratory.

Acknowledgements

This work was supported by grants from the MIUR (Rome, Italy) and the FIRB-Futuro-in-Ricerca project RBFR1022UQ: “Novel Au(I)-based molecular catalysts: from know-how to know-why (AuCat)”.

Notes and references

^a Dipartimento di Chimica, Fisica e Ambiente, Università di Udine, Via Cotonificio 108, I-33100 Udine, Italy;

^b Istituto di Scienze e Tecnologie Molecolari del CNR (CNR-ISTM), c/o Dipartimento di Chimica, Università degli Studi di Perugia, via Elce di Sotto 8, I-06123, Perugia, Italy;

^c Dipartimento di Dipartimento di Chimica, Biologia e Biotecnologie, Università degli Studi di Perugia Via Elce di sotto 8, I-06123, Perugia, Italy;

These authors contributed equally to this work.

† Electronic Supplementary Information (ESI) available: experimental section and computational studies. See DOI: 10.1039/b000000x/

¹ A. Macchioni, *Chem. Rev.* 2005, **105**, 2039-2073 and reference therein

² (a) B. Binotti, G. Bellachioma, C. Cardaci, C. Carfagna, C. Zuccaccia, A. Macchioni, *Chem. Eur. J.* 2007, **13**, 1570–1582. (b) P. G. A. Kumar, P. S. Pregosin, M. Vallet, G. Bernardinelli, R. F. Jazzar, F. Viton, E. P. Kündig, *Organometallics* 2004, **23**, 5410-5418. (c) A. Moreno, P. S. Pregosin, G. Laurenczy, A. D. Phillips, P. J. Dyson, *Organometallics* 2009, **28**, 6432-6441 (d) D. Sirbu, G. Consiglio, B. Milani, P. G. A. Kumar, P. S. Pregosin, S. Gischig, *J. Organomet. Chem.* 2005, **690**, 2254–2262.

³ A. S. K. Hashmi, *Chem. Rev.* 2007, **107**, 3180-3211.

⁴ A. Corma, A. Leyva-Pérez, M. J. Sabater, *Chem. Rev.* 2011, **111**, 1657-1712.

⁵ D. J. Gorin, B. D. Sherry, F. D. Toste, *Chem. Rev.* 2008, **108**, 3351-3378.

⁶ A. Corma, V. R. Ruiz, A. Leyva-Pérez, M. J. Sabater, *Adv. Synth. Catal.* 2010, **352**, 1701-1710.

⁷ G. Henrion, T. E. J. Chavas, X. Le Goff, F. Gagosz, *Angew. Chem. Int. Ed.* 2013, **52**, 6277-6282.

⁸ (a) C. Brouwer, C. He, *Angew. Chem. Int. Ed.* 2006, **45**, 1744-1747; (b) R. Gramage-Doria, R. Bellini, J. Rintjema, J. N. H. Reek, *ChemCatChem* 2013, **5**, 1084-1087; (c) A. Homs, C. Obradors, D. Lebeuf, A. M. Echavarren, *Adv. Synth. Catal.* 2014, **356**, 221–228

⁹ (a) Y. Xia, A. S. Dudnik, V. Gevorgyan, Y. Li, *J. Am. Chem. Soc.* 2008, **130**, 6940; (b) M. Jia, G. Cera, D. Perrotta, M. Monari, M. Bandini, *Chem. Eur. J.* 2014, **20**, 9875-9878 (c) Z. Zhang, C. Liu, R. E. Kinder, X. Han, H. Qian, R. A. Widenhofer, *J. Am. Chem. Soc.* 2006, **128**, 9066-9073

¹⁰ (a) G. L. Hamilton, E. J. Kang, M. Mba, F. D. Toste, *Science* 2007, **317**, 496. (b) R. L. LaLonde, B. D. Sherry, E. J. Kang, F. D. Toste, *J. Am. Chem.*

- Soc. 2007, **129**, 2452. (c) M. Bandini, A. Bottoni, M. Chiarucci, G. Cera, G. P. Miscione, *J. Am. Chem. Soc.* 2012, **134**, 20690-20700
- ¹³ K. Aikawa, M. Kojima, K. Mikami, *Angew. Chem. Int. Ed.* 2009, **48**, 6073-6077.
- ¹² D. Weber, T. D. Jones, L. Adduci, M. R. Gagnè, *Angew. Chem. Int. Ed.* 2012, **51**, 1-6. (b) V. M. Lau, C. F. Gorin, M. W. Kanan, *Chem. Sci.* 2014, DOI: 10.1039/C4SC02058H
- ¹³ A. S. K. Hashmi, *Nature* 2007, **449**, 292.
- ¹⁴ D. Zuccaccia, L. Belpassi, F. Tarantelli, A. Macchioni, *Eur. J. Inorg. Chem.* 2013, **24**, 4121-4135.
- ¹⁵ G. Bellachioma, G. Ciancaleoni, C. Zuccaccia, D. Zuccaccia, A. Macchioni, *Coord. Chem. Rev.* 2008, **252**, 2224-2238.
- ¹⁶ (a) G. Ciancaleoni, L. Belpassi, F. Tarantelli, D. Zuccaccia, A. Macchioni, *Dalton Trans.* 2013, **42**, 4122-4131; (b) D. Zuccaccia, L. Belpassi, L. Rocchigiani, F. Tarantelli, A. Macchioni, *Inorg. Chem.* 2010, **49**, 3080-3082. (c) N. Salvi, L. Belpassi, D. Zuccaccia, F. Tarantelli, A. Macchioni, *J. Organomet. Chem.* 2010, **695**, 2679-2686. (d) G. Ciancaleoni, L. Biasiolo, G. Bistoni, A. Macchioni, F. Tarantelli, D. Zuccaccia, L. Belpassi, *Organometallics* 2013, **32**, 4444-4447. (e) D. Zuccaccia, L. Belpassi, F. Tarantelli, A. Macchioni, *J. Am. Chem. Soc.* 2009, **131**, 3170-3171
- ¹⁷ (a) C. Zuccaccia, A. Macchioni, I. Orabona, F. Ruffo *Organometallics* 1999, **18**, 4367-4372. (b) A. Macchioni, A. Magistrato, I. Orabona, F. Ruffo, U. Rothlisberger, C. Zuccaccia *New. J. Chem.* 2003, **27**, 455-458. (c) G. Bellachioma, B. Binotti, G. Cardaci, C. Carfagna, A. Macchioni, S. Sabatini, C. Zuccaccia, *Inorg. Chim. Acta* 2002, **330**, 44-51
- ¹⁸ (a) R. Romeo, N. Nastasi, L. Mosù Scolaro, M. R. Plutino, A. Albinati, A. Macchioni, *Inorg. Chem.* 1998, **37**, 5460-5466. (b) D. Zuccaccia, A. Macchioni, *Organometallics* 2005, **24**, 3476-3486. (c) L. Ion, D. Morales, J. Pérez, L. Riera, V. Riera, R. A. Kowenicki, M. McPartlin *Chem. Commun.* 2006, 91-93.
- ¹⁹ L. Biasiolo, M. Trinchillo, P. Belanzoni, L. Belpassi, V. Busico, G. Ciancaleoni, A. D'Amora, A. Macchioni, F. Tarantelli, D. Zuccaccia *Chem. Eur. J.* 2014, **20**, 14594-14598
- ²⁰ A. Zhdanko, M. E. Maier, *ACS Catal.* 2014, **4**, 2770-2775
- ²¹ J. H. Teles, S. Brode, M. Chabanas, *Angew. Chem. Int. Ed.* 1998, **37**, 1415-1417
- ²² (a) Teles, J. H. in "Modern Gold catalyzed synthesis" Edited by A. S. K. Hashmi, F. D. Toste, 2012, Wiley. (b) A. S. K. Hashmi, M. Bührle *Aldrichimica Acta* 2010, **43**, 27-33 (c) K. Graf, P. D. Hindenberg, Y. Tokimizu, S. Naoe, M. Rudolph, F. Rominger, H. Ohno, A. S. K. Hashmi *ChemCatChem* 2014, **6**, 199-204 (d) A. S. K. Hashmi, I. Braun, M. Rudolph, F. Rominger *Organometallics* 2012, **31**, 644-661.
- ²³ (a) G. Kovács, G. Ujaque, A. Lledós, *J. Am. Chem. Soc.*, 2008, **130**, 853-864. (b) A. S. K. Hashmi, I. Braun, M. Rudolph, F. Rominger *ChemCatChem* 2010, **2**, 1226-1230.
- ²⁴ L. M. Slaughter, *ACS catal.* 2012, **2**, 1802
- ²⁵ (a) C. Bartolomé, Z. Ramiro, P. Pérez-Galán, C. Bour, M. Raducan, A.M. Echavarren, P. Espinet, *Inorg. Chem.* 2008, **47**, 11391. (b) C. Nieto-Oberhuber, S. López, A.M. Echavarren, *J. Am. Chem. Soc.* 2005, **127**, 6178. (c) C. Bartolomé, Z. Ramiro, D. García-Cuadrado, P. Pérez-Galán, M. Raducan, C. Bour, A. M. Echavarren, P. Espinet, *Organometallics* 2010, **29**, 951. (d) C. Bartolomé, D. García-Cuadrado, Z. Ramiro, P. Espinet, *Organometallics* 2010, **29**, 3589. (e) C. Bartolomé, D. García-Cuadrado, Z. Ramiro, P. Espinet, *Inorg. Chem.* 2010, **49**, 9758. (f) A.S.K. Hashmi, T. Hengst, C. Lothschütz, F. Rominger, *Adv. Synth. Catal.* 2010, **352**, 1315. (g) H. Seo, B. P. Roberts, K. A. Abboud, K. A. Merz Jr., S. Hong, *Org. Lett.* 2010, **12**, 4860. (h) H. Seo, D. R. Snead, K. A. Abboud, S. Hong, *Organometallics* 2011, **30**, 5725. (i) A. S. K. Hashmi, T. Haffner, M. Rudolph, F. Rominger, *Eur. J. Org. Chem.* 2011, 667. (l) A. S. K. Hashmi, T. Haffner, M. Rudolph, F. Rominger, *Chem. Eur. J.* 2011, **17**, 8195. (m) C. F. Bender, R. A. Widenhofer, *Org. Lett.* 2006, **8**, 5303. (n) Y.M. Wang, C. N. Kuzniewski, V. Rauniyar, C. Hoong, F. D. Toste, *J. Am. Chem. Soc.* 2011, **133**, 12972. (o) M. C. Blanco Jaimés, C. R. N. Bçhling, J. M. Serrano-Becerra, A. S. K. Hashmi, *Angew. Chem. Int. Ed.* 2013, **52**, 1-5.
- ²⁶ V. Amendola, L. Fabbrizzi, L. Mosca, *Chem. Soc. Rev.* 2010, **39**, 3889-3915 and reference therein
- ²⁷ K. A. Schug, W. Lindner, *Chem. Rev.* 2005, **105**, 67-113 and references therein.
- ²⁸ L. Belpassi, I. Infante, F. Tarantelli, L. Visscher, *J. Am. Chem. Soc.* 2008, **130**, 1048-1060.
- ²⁹ G. Bistoni, L. Belpassi, F. Tarantelli, *Angew. Chem. Int. Ed.* 2013, **52**, 11599-11602
- ³⁰ NOE intensities must be scaled considering that they are proportional to $(n_i \cdot n_s / n_i + n_s)$, where n_i and n_s are the number of equivalent I and S nuclei (that undergo a dipolar interaction), respectively. See: S. Macura, R. R. Ernst, *Mol. Phys.* 1980, **41**, 95.
- ³¹ A. Zhdanko, M. E. Maier, *Chem.-Eur. J.*, 2014, **20**, 1918-1930.
- ³² Assuming that the minimum distance between the anion and the cation is the same in both the orientations, the abundances have been estimated by the normalized NAC/anion and alkyne/anion NOE intensities. For the NAC-side orientation the protons showing the largest NOEs have been selected as the probes instead of the sum of the intensities in the assumption that a single anion orientation is present on the side of the ligand, while H2 have been chosen as the probes of the alkyne side orientation.
- ³³ E. A. Kataev, C. Müller, G. V. Kolesnikov, V. N. Khurstalev, *Eur. J. Org. Chem.*, 2014, 2747-2753.
- ³⁴ W. Wang, G. B. Hammond, B. Xu, *J. Am. Chem. Soc.* 2012, **134**, 5697-5705.
- ³⁵ D. Zuccaccia, G. Bellachioma, G. Cardaci, G. Ciancaleoni, C. Zuccaccia, E. Clot, A. Macchioni, *Organometallics*, 2007, **26**, 3930-3946.
- ³⁶ This assumption cannot be verified because the $[LAu(3\text{-hexyne})]^+$ cannot be studied in methanol since it undergoes nucleophilic attack from the solvent.

Graphical Abstract

The role of the ligand in determining the ion pair structure of the $[(\text{NAC})\text{Au}(\eta^2\text{-3-hexyne})]^+ \text{BF}_4^-$ catalysts and how the position of the anion (position A, B and C) influences their catalytic performances in the intermolecular alkoxylation of alkynes, have been studied.

